Inorganica Chimica Acta 450 (2016) 236–242

Contents lists available at ScienceDirect

Inorganica Chimica Acta

journal homepage: www.elsevier.com/locate/ica

Research paper

Metal nitrosyl chemistry: Interesting oxidation and nitrosylation of a metal-bound ligand framework in a diamido-bis(phosphine) ruthenium (II) complex

Daniel N. Huh [b], Eric T. Czer [c], Kyle E. Cordova [d], Wesley I. Chow [e], Curtis E. Moore [a], Arnold L. Rheingold [a], Christopher J.A. Daley [e,*]

[a] Department of Chemistry and Biochemistry, University of California – San Diego, 9500 Gillman Drive, La Jolla, CA 92093, United States
[b] Department of Chemistry, University of California – Irvine, Irvine, CA 92697, United States
[c] Kansas City University of Medicine and Biosciences, 1750 Independence Ave, Kansas City, MO 64106, United States
[d] Berkeley Global Science Institute, BG6 Giauque Hall, Berkeley, CA 94720, United States
[e] Department of Chemistry and Biochemistry, University of San Diego, 5998 Alcala Park, San Diego, CA 92110, United States

ARTICLE INFO

Article history:
Received 13 January 2016
Received in revised form 1 June 2016
Accepted 2 June 2016
Available online 3 June 2016

Keywords:
Ruthenium-diamido and diimino-bis (phosphine) complexes
X-ray crystal structures
Nitric oxide
Metal-activated nitrosylation
Dioxime

ABSTRACT

The complex Ru((*R*,*R*)-DACH-Naph)Cl_2 ((*R*,*R*)-**2**), a neutral Ru(II) complex of the Trost diamido-bis(phosphine) ligand ((*R*,*R*)-DACH-Naph (H_2**1**)) was synthesized in 86% yield via the direct stoichiometric reaction of H_2**1** and $RuCl_2(DMSO)_4$ in refluxing toluene. Complex (*R*,*R*)-**2** was further reacted with excess [NO][BF_4] producing Ru($(HON)_2$-DICH-Naph)Cl_2 (**4**) in 48% yield; a Ru(II) complex where the Trost ligand has been oxidized to a diimine and nitrosylated, on the backbone cyclohexyl ring, to a dioxime. The structures of (*R*,*R*)-**2** and **4** were revealed in the solid state by single-crystal X-ray analysis and in the solution state via ^{1}H NMR spectroscopy.

1. Introduction

Nitric oxide (NO) is a critical signaling molecule for several important biological processes [1–6]. As such, the chemistry of NO and NO-containing compounds has garnered significant attention [7–9]. One area of intense investigation has been the reaction of NO at metal centers in several enzymes. Studies of NO reactivity with metal complexes have yielded significant information about metal-NO chemistry and have resulted in the development of metal-based NO-sensor and NO–scavenger technologies [10–13]. More recently, transition metal-NO complexes have been developed that act as NO donors through the release of coordinated NO upon exposure to light, which are of significant interest in the medical industry [14,15]. Ideally, such systems could be developed as light controlled, site-specific NO delivery systems to a cellular target.

To date, a number of successful efforts to develop photosensitive metal nitrosyl complexes have been reported. In particular, the Maschark group has developed a series of transition metal-NO complexes that have shown significant promise with some being both thermally stable in biological media and capable of rapidly releasing NO on exposure to low-intensity (mW) UV light [16]. Many successful complexes reported by the Mascharak group have contained tetradentate or pentadentate nitrogen- or mixed nitrogen/oxygen-based coordinating ligand systems with only one example of a phosphine-based ligand system being reported. The latter study was on a ruthenium complex derived from the tetradentate dicarboxamide-bis(phosphine) ligand 1,2-bis-*N*-[2′(diphenyl-phosphanyl)benzoyl]diaminobenzene (**A**: $dppbH_2$) [17a]. The complex was determined to be ineffective owing to two factors: (1) unwanted ligand oxidation on preparation of the desired Ru(III) deprotonated dicarboxamido-bis(phosphine) complex (Ru(dppb)), resulting in the formation of the Ru(II) diimine-bis(phosphine) complex Ru(dppQ)Cl_2 (**B**: dppQ: 1,2-bis-*N*-[2′(diphenylphosphanyl) benzoyl]diiminocyclohexa-3,5-diene) and (2) unwanted nitration of the activated ligand-backbone on reaction of Ru(dppQ)Cl_2 with NO (**C**).

* Corresponding author.
E-mail address: cjdaley@sandiego.edu (C.J.A. Daley).

http://dx.doi.org/10.1016/j.ica.2016.06.001
0020-1693/

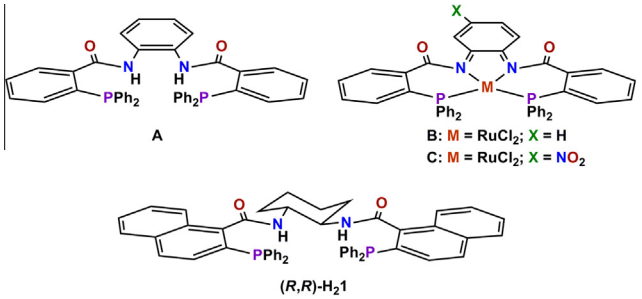

Our group has been investigating dicarboxamide-dithiol and dicarboxamide-bis(phosphine) ligand systems as ligand architectures to prepare active-site synthetic analogues of nitrile hydratase and related enzymes. Stemming from our work and that reported by Mascharak, we investigated ruthenium-nitrosyl chemistry using the well-known Trost dicarboxamido-bis(phosphine) ligand system. Herein, we describe our findings: (1) the synthesis and characterization of Ru(II)((*R*,*R*)-H_2**1**)Cl_2 ((*R*,*R*)-**2**), where H_2**1** is Trost's 1,2-bis-*N*-[2′(diphenylphosphanyl)naphthoyl]-diaminocyclohexane ligand (DACH-Naph) – containing two potentially deprotonatable carboxamido protons, and (ii) the resulting products of reaction of (*R*,*R*)-**2** with [NO][BF_4] in attempts to prepare a Ru-NO complex.

2. Materials and methods

2.1. Reagents and techniques

All reagents were purchased from commercial sources and used as received. Solvents (Et_2O, DMF, and CH_2Cl_2) were dried by passing through an Innovative Technologies solvent purification system and collected just prior to use and further deoxygenated by bubbling with a stream of N_2 for 30 min prior to use. NMR spectra were collected on a 400 MHz or 500 MHz Varian NMR spectrometer and chemical shifts, integration, and coupling constant analyses were performed using MestReNova (version 5.2.5) software. ^{1}H NMR chemical shifts are referenced to TMS. ^{31}P{^{1}H} NMR chemical shifts are referenced to 85% $H_3PO_{4(aq)}$. UV–vis spectroscopy was performed on a Cary 50 at room temperature in 1.0 cm cells. FTIR analyses were performed on a Jasco Ft/IR-480 Plus spectrometer as thin films on a NaCl salt plate or as a solution in a Wilmad permanent sealed 0.10 mm NaCl liquid cell. Elemental analysis was performed at Micro-Analysis, Inc. (Wilmington, DE, 19808). High resolution mass spectrometry (TOF-MS ES$^+$) analysis was performed at the Mass Spectrometry Facility of the University of California, Irvine (Irvine, CA, 92697). The compounds $RuCl_2(DMSO)_4$ (Strem), (*R*,*R*)-1,2-bis-*N*-[2′(diphenylphosphanyl)naphthoyl]-diaminocyclohexane (((*R*,*R*)-DACH-Naph: Strem) and [NO][BF_4] (Aldrich) were purchased from commercial sources and used as received. ^{1}H NMR of commercial (*R*,*R*)-DACH-Naph was assigned via multinuclear NMR for analysis purposes ((500 MHz, $CDCl_3$, rt): δ 7.82 (H_f: d, J = 8.5, 2H), 7.73 (H_i: d, J = 8.2, 2H), 7.69 (H_j: d, J = 8.5, 2H), 7.37 (H_h: "t", J = 7.5, 2H), 7.34 (Ph: m, 8H), 7.27 (Ph: m, 8H), 7.20 (Ph: br t, J = 7.4, 4H), 7.05 (H_k: dd, J = 8.5, 3.0, 2H), 7.01 (H_g: br t, J = 7.5, 2H), 6.54 (N*H*: br d, 2H), 3.81 (Ha: br m, 2H), 2.33 (H_b: br d, J = 12.1, 2H), 1.70 (H_d: br m, 2H), 1.29 (H_e: br t, 2H), 1.21 (H_c: br m, 2H); labels correspond with those shown for ligand framework of (*R*, *R*)-**2** in Fig. 2) as well as FTIR (thin film; 3398 cm^{-1} (s, ν_{N-H}), 1649 cm^{-1} (s, $\nu_{C=O}$)).

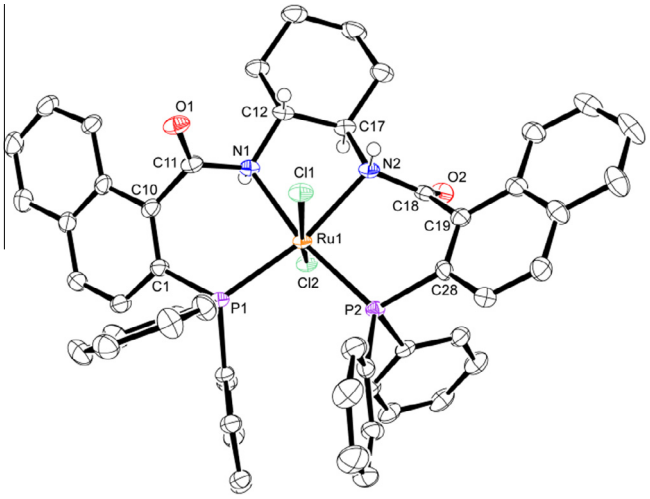

Fig. 1. Molecular structure of Ru((*R*,*R*)-H_2**1**)Cl_2 ((*R*,*R*)-**2**) showing ellipsoids at the 50% probability level and atom labeling scheme. All H atoms except those of the amine and chiral carbon centers (N1, N2, C12 and C17) are omitted for clarity.

2.2. Syntheses

2.2.1. Synthesis of (R,R)-2

To a 100 mL side-arm flask was added the ligand (*R*,*R*)-1,2-bis-*N*-[2′(diphenylphosphanyl)-naphthoyl]-diaminocyclohexane ((*R*,*R*)-DACH-Naph; (*R*,*R*)-H_2**1**: 151.6 mg, 1.917×10^{-4} mol), $RuCl_2(DMSO)_4$ (94.1 mg, 1.94×10^{-4} mol), and a magnetic stir bar. To this was added toluene (30 mL) via cannula. The reaction flask was equipped with a reflux condenser and the heterogeneous mixture was stirred and heated to reflux (110 °C) for 14 h. The yellow colored heterogeneous mixture turns homogeneous after several hours of heating becoming dark orange in color. After further heating, the product, (*R*,*R*)-**2**, begins to precipitate from solution. After heating, the solution was cooled in an ice bath to complete the precipitation of the product. The solution was inverse-filtered, the solid was washed with toluene (3×5 mL) and dried under high vacuum to give the orange (*R*,*R*)-**2** (158.0 mg, 1.646×10^{-4} mol) in 86% yield.

FTIR (thin film, rt) cm^{-1}: 3420 (s, ν_{N-H}), 1721 (s, $\nu_{C=O}$). UV–vis (CH_2Cl_2, rt): λ_{max} (ε) = 486 nm (275). Combustion analysis (calculated, observed): C 64.87, 64.40; H 4.61, 4.62; N 2.91, 2.80. HRMS (TOF-MS ES$^+$) observed (theoretical): [M + Na]$^+$ 985.1195 (985.1205). ^{1}H NMR (500 MHz, $CDCl_3$, rt): δ 8.10 (H_f: d, J = 8.4, 2H), 7.84 (H_i: d, J = 7.8, 2H), 7.74 (H_j: d, J = 8.7, 2H), 7.60 (H_g, H_h, N*H*: m, 6H), 7.37 (p_2-Ph: t, J = 7.5, 2H), 7.16 (p_1-Ph: t, J = 7.3, 2H), 7.05 (H_k, m_2-Ph: m, 6H), 7.00 (m_1-Ph: t, J = 7.3, 4H), 6.92 (o_1-Ph: br m, 4H), 4.29 (Ha: br m, 2H), 2.88 (H_b: br m, 2H), 1.90 (H_d: br m, 2H), 1.45 (H_c, H_e: br m, 4H); ^{31}P{^{1}H} NMR (260 MHz, $CDCl_3$, rt): δ 47.6 (s).

2.2.2. Synthesis of 4

To a 50 mL Schlenk tube equipped with a stirbar was added (*R*,*R*)-**2** (63.0 mg, 6.54×10^{-5} mol) and DMF (8 mL) and the flask was cooled to −30 °C in an acetone/dry ice bath. To the pale orange suspension, a solution of [NO][BF_4] (86.7 mg, 7.42×10^{-4} mol) in DMF (3 mL) was added via cannula. On stirring, the color of the solution turned deep purple within 5 min. The reaction mixture was left to stir for 20 h. Dark purple-black precipitate of **4** was isolated via inverse-filtration of the reaction mixture, where the filtrate was kept and collected in a 50 mL side-arm flask. The precipitate was washed with Et_2O (2×3 mL) and dried under high vacuum for 24 h. The original filtrate solution in the 50 mL side-arm flask was layered with Et_2O (40 mL) and left to crystallize at room temperature for 48 h. Micro-crystals were observed and collected by inverse filtration and combined with first crop to yield **4** (32 mg, 3.1×10^{-5} mol) in a 48% yield. FTIR (dilute CH_3CN solution, rt)

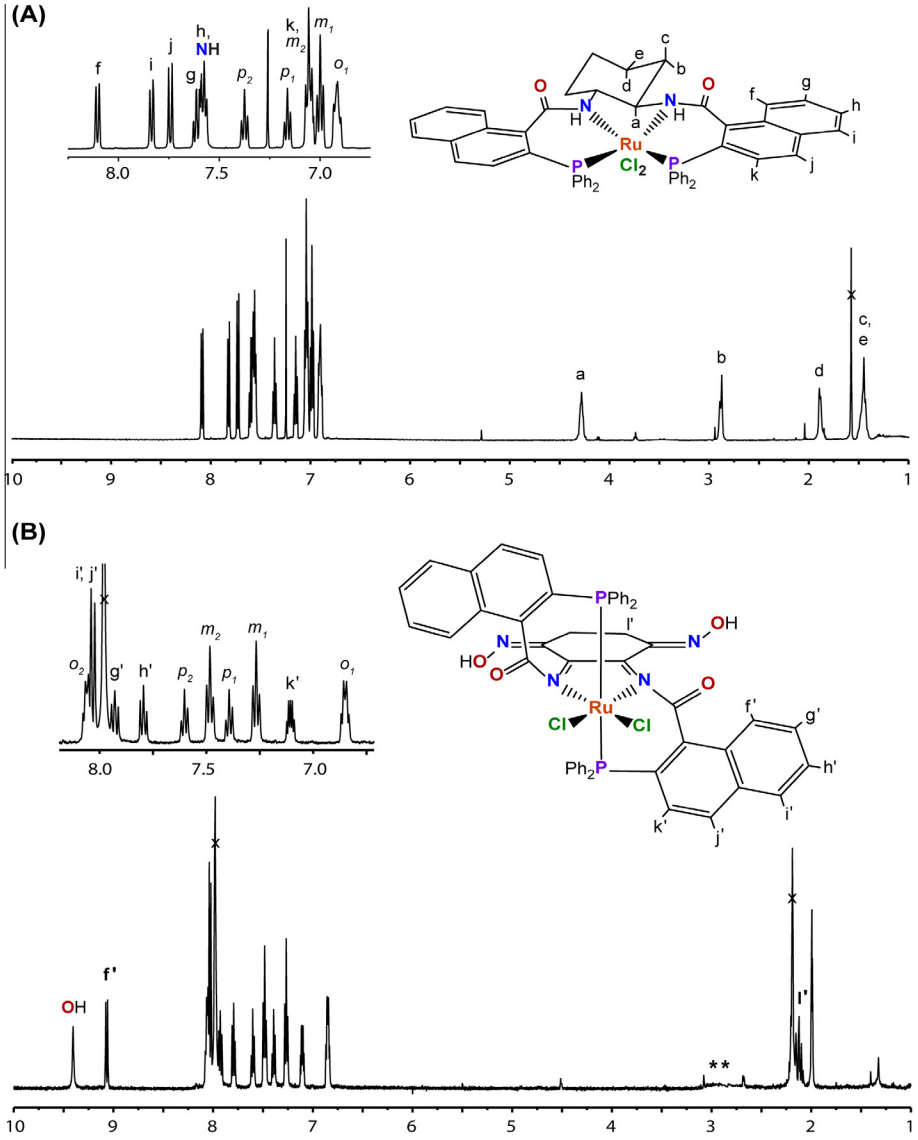

Fig. 2. ^{1}H NMR spectra of (*R*,*R*)-**2** and **4**: (A) Ru((*R*,*R*)-H_2**1**)Cl_2 ((*R*,*R*)-**2**) in $CDCl_3$ and (B) Ru((HON)$_2$-DICH-Naph)Cl_2 (**4**) in MeCN-d_3. Residual solvents denoted with 'x': DMF and, or H_2O. Signals for the methyl groups of DMF (denoted by *s) in (B) were suppressed using PRESAT on vjnmr. Structures of (*R*,*R*)-**2** and **4** are depicted with the Cl ligands of (*R*,*R*)-**2** not drawn in their apical positions for clarity of proton labels. ^{1}H NMR proton assignments, which were determined via multinuclear NMR experiments, are shown. Signals for the second set of ortho-phenyl protons (Ho_2) in (*R*,*R*)-**2** were not observed.

cm^{-1}: 3630 (s, ν_{O-H}), 3542 (s, ν_{O-H}), 1677 (s, $\nu_{C=O}$), 1632 (s, $\nu_{C=N}$). UV–vis (CH_3CN, rt): λ_{max} (ε) = 530 nm (1250), 405 nm (1350). HRMS (TOF-MS ES$^+$) observed (theoretical): $[M + Na]^+$ 1039.0682 (1039.0696). ^{1}H NMR (500 MHz, CDCN, rt): δ 9.35 (O*H*: br s, 2H), 9.02 (H_f: d, J = 8.9, 2H), 8.01 (o_2-Ph: br q, 4H), 7.98 ($H_{i'}$, $H_{j'}$: br d, J = 8.5, 4H), 7.88 ($H_{g'}$: br dd, 2H), 7.74 ($H_{h'}$: t, J = 7.5, 2H), 7.55 (p_2-Ph: t, J = 7.4, 2H), 7.43 (m_2-Ph: t, J = 7.6, 4H), 7.34 (p_1-Ph: t, J = 7.5, 2H), 7.21 (m_1-Ph: t, J = 7.6, 4H), 7.05 ($H_{k'}$: dt, J = 8.5, 4.3, 2H), 6.80 (o_1-Ph: br q, 4H), 2.15 ($H_{l'}$: m, 4H); ^{31}P{^{1}H} NMR (260 MHz, $CDCl_3$, rt): δ 24.8 (s).

2.3. Crystallography measurements

X-ray quality crystals of (*R*,*R*)-**2** were grown from a concentrated CH_2Cl_2 solution via vapor diffusion with Et_2O while crystals of **4** were grown from a concentrated DMF solution via vapor diffusion with Et_2O. Data for (*R*,*R*)-**2** and **4** were collected at the University of California San Diego on a Bruker Kappa APEX II CCD diffractometer equipped with Mo K_α radiation (λ = 0.71073). The crystals were mounted on a Cryoloop with Paratone oil and data were collected in a nitrogen gas stream at 100(2) K using ϕ and ω scans. The data were integrated using the Bruker SAINT [18] software program and scaled using the SADABS [19] software program. The structures were solved using direct methods (SHELXS). [20] The SQUEEZE [21] program was used to account for solvent disorder in (*R*,*R*)-**2** (0.5 × CH_2Cl_2, 0.5 × Et_2O) and **4** (4 × DMF).

All non-hydrogen atoms were refined anisotropically by full-matrix least-squares (SHELXL). [20] The carboxamide hydrogen atoms of (*R*,*R*)-**2** were found via the difference map and the bond distance was restrained relative to the parent oxygen atom using the appropriate DFIX command in SHELXL. All other hydrogen atoms were placed using a riding model. Their positions were constrained relative to their parent atom using the appropriate HFIX command in SHELXL. Crystallographic data are summarized in Table 1.

Table 1
Crystallographic data of compounds (*R*,*R*)-**2**, and **4**.[a]

	(*R*,*R*)-**2** · 0.5 CH_2Cl_2 · 0.5 Et_2O	**4** · 4 DMF
Formula	$C_{54.5}H_{50}Cl_3N_2O_{2.5}P_2Ru$	$C_{64}H_{66}Cl_2N_8O_8P_2Ru$
Formula weight	1042.32	1309.15
Crystal dimensions (mm)	0.23 × 0.13 × 0.08	0.25 × 0.20 × 0.15
Crystal system	Hexagonal	Monoclinic
Space group	*P6₁*	*P2/n*
Unit cell parameters[a]		
a (Å)	21.2986 (14)	14.6744 (4)
b (Å)	21.2986 (14)	10.9784 (3)
c (Å)	20.5703 (14)	18.4169 (5)
α (deg)	90	90
β (deg)	90	92.1900 (10)
λ (deg)	120	90
V (Å^3)	8081.2 (12)	2964.82 (14)
Z	6	2
D_{calc} (g cm^{-3})	1.285	1.466
μ (mm^{-1})	0.540	0.473
Radiation (λ [Å])	Mo Kα (0.71073)	Mo Kα (0.71073)
Temperature (°C)	100 (2)	100 (2)
2θ range data collection (deg)	2.153–28.315	2.545–29.568
No. reflections collected	113,668	26,681
No. independent reflections	12,740 [R_{int} = 0.0469]	7338 [R_{int} = 0.0307]
Data/restraints/parameters	12,740/1/550	7338/0/303
GoF[b]	1.088	1.087
Final *R* indices		
R_1[c]	0.0314	0.0391
wR_2[d]	0.0687	0.0976
Largest Δ peak/hole (e Å^{-3})	0.413, −0.255	0.598, −0.845

[a] See CCDC-1445800 ((*R*,*R*)-**2**) and CCDC-1445801 (**4**) structure files for more information.
[b] GoF = $[\Sigma w(F_o^2 - F_c^2)^2/(N_{data} - N_{params})]^{1/2}$.
[c] $R_1 = \Sigma||Fo| - |Fc||/\Sigma|Fo|$.
[d] $wR_2 = [\Sigma w(F_o^2 - F_c^2)^2/\Sigma w(F_o^4)]^{1/2}$.

3. Results and discussion

3.1. Synthesis of Ru((*R*,*R*)-H_2**1**) (**2**) using Trost's naphthyl diamidato-bis(phosphine) ligand ((*R*,*R*)-DACH-Naph: (*R*,*R*)-H_2**1**)

A heterogeneous 1:1 mixture of $Ru(DMSO)_4Cl_2$ and the DACH-Naph Trost ligand (*R*,*R*)-H_2**1** was reacted in toluene at 110 °C. Over a few hours of heating the mixture became homogeneous which, on further heating overnight, precipitated orange-red powder of [Ru((*R*,*R*)-H_2**1**)Cl_2] ((*R*,*R*)-**2**) from solution. Complete precipitation of the product occurred on cooling the solution to room temperature as indicated by the lack of any significant orange-red color in the solution phase (Scheme 1: 86% yield).

The structure of (*R*,*R*)-**2** in the solid and solution states was confirmed by X-ray crystallography and NMR spectroscopy, respectively. Single crystals of (*R*,*R*)-**2** were grown from a concentrated CH_2Cl_2 solution via vapor diffusion with Et_2O and the X-ray structure is depicted in Fig. 1. The program SQUEEZE was used to account for disordered co-crystallized solvent modeled as 0.5 CH_2Cl_2 and 0.5 Et_2O per molecule of (*R*,*R*)-**2**. The enantiopurity of (*R*,*R*)-**2** was confirmed from the determined Flack (χ) parameter value of −0.008(13). The coordination sphere around the ruthenium center is octahedral with the ligand (*R*,*R*)-H_2**1** occupying a tetradentate plane having neutral diamido, *cis*-bis(phosphine) coordination. This coordination is in contrast to the similar achiral Ru(dppQ)Cl_2 complex reported by Mascharak [17a], which contains *trans*-phosphine coordination. The dppQ ligand has also been reported to bind to Pd both in its neutral form as a bidentate trans-spanning bis(phosphine) complex [17c], and its dianionic form as a planar tetradentate diamidato-bis(phosphine) complex [17b], the latter of which has also been reported for the platinum analogue [17a]. With respect to H_2**1**, planar-tetradentate ligand coordination of (*R*,*R*)-H_2**1** has been observed in Pd and Pt metal complexes when bound in its doubly-deprotonated form [22] but, to the best of our knowledge, this is the first report of H_2**1** being bound in its neutral tetradentate form. The observed Ru–P and Ru–Cl bond lengths in (*R*,*R*)-**2** (Ru–P: 2.296, 2.291 Å; Ru–Cl: 2.412, 2.399 Å) are consistent with those in Ru(dppQ)Cl_2 (Ru–P: 2.358 and 2.359 Å; Ru–Cl: 2.409, 2.407 Å) and the Ru–N bond lengths (2.239 and 2.236 Å) are consistent for neutral *N*-carboxamido coordination.

X-ray analysis indicates that (*R*,*R*)-**2** is not C_2-symmetric in the solid state however, in solution, ^{31}P NMR analyses indicate that it behaves as a C_2-symmetric system as only one signal is observed at δ 47.6 (s). ^{1}H NMR analysis confirms the finding with the number of signals observed being half those expected for an asymmetric complex (Fig. 2A). Proton assignments were determined via multinuclear NMR experiments and correlate well with our previous reported studies on Pt((*R*,*R*)-**1**) and Pd((*R*,*R*)-**1**) where the amide protons of (*R*,*R*)-H_2**1** are deprotonated [22]. Specifically, we noted the shifted downfield signal at δ 8.10 is characteristic of the naphthyl proton (H_f) on coordination of the amide-nitrogen to a metal center. Note, all protons were accounted for except for one C_2-symmetric set of *ortho*-phenyl protons (Ho_2), which were not observed. Analysis of ^{1}H NMR spectra taken at a few different relaxation times did not reveal any significant changes, with the total integration being short by 4 protons (the set of C_2-symmetric *ortho*-Ph protons) in all cases. We do not have concrete reasoning for the lack of signal, however all analytical data acquired including HRMS and X-ray crystallography support the structure. Furthermore, FTIR analysis indicated the presence of N–H bonding (ν_{NH}: 3420 cm^{-1}) as well as the expected shifting of the carbonyl stretch, ν_{CO}, to higher wavenumber on coordination of the amide-nitrogen in (*R*,*R*)-**2** (1721 cm^{-1}) relative to that of the free ligand (*R*,*R*)-H_2**1** (1649 cm^{-1}) owing to the lack of resonance in the former as the nitrogen lone-pair electrons are occupied in the N–Ru bonding.

3.2. Synthesis of Ru(N_2P_2-$(NOH)_2$) (**4**) using [NO][BF_4] as oxidant and nitrosylation reagent

Attempts to prepare a Ru(III)–NO complex were undertaken by reacting (*R*,*R*)-**2** with 1 equiv of [NO][BF_4] in anticipation of forming a Ru–NO bond with concurrent oxidation of the ruthenium center to Ru(III) [23]. Analysis of the NMR spectra of the reaction indicated numerous products present in solution including unreacted starting material. On reaction of (*R*,*R*)-**2** with excess [NO][BF_4], the product mixture was less complicated with only one major phosphorus containing ruthenium species being present as determined by ^{31}P NMR. The crude product was isolated in 48% yield and single crystals were grown via vapor diffusion of Et_2O into a concentrated DMF solution of the complex. X-ray analysis confirmed the product was not a Ru–NO complex but rather Ru($(HON)_2$-DACH-Naph)Cl_2 (**4**) (Fig. 3); an oxidized- and nitrosylated-ligand complex of Ru(II).

Unlike in the case with (*R*,*R*)-**2**, **4** behaves as a C_2-symmetric system in both the solid and solution states. Complex **4** crystallized in the *P2/n* point group with the ruthenium metal center located at a C_2 special position. Four equivalents of DMF co-crystallized with **4** but they were severely disordered thus SQUEEZE [21] was used to account for the solvent residual density. The structure of **4** was well-resolved, with only minor conformational disorder in the cyclohexyldiimine dioxime ring system that was successfully modeled in two conformations in a 60:40 ratio with the major form depicted in Fig. 3. The overall geometry around the

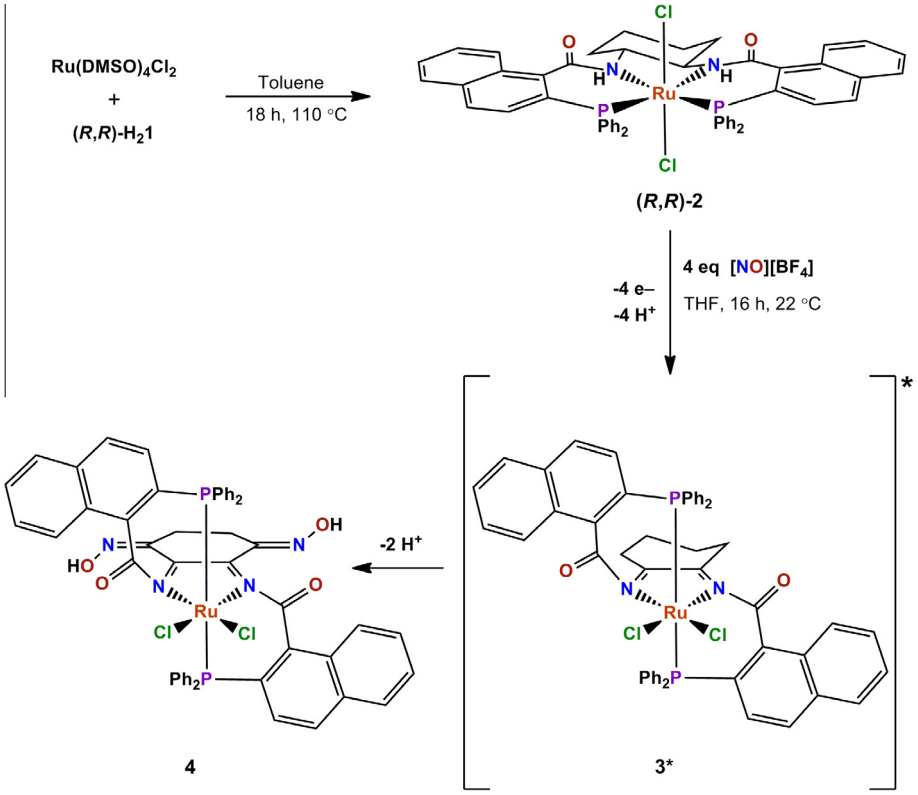

Scheme 1. Proposed synthetic pathway from ruthenium complex (*R*,*R*)-**2** to nitrosylated complex **4** through proposed intermediate **3***.

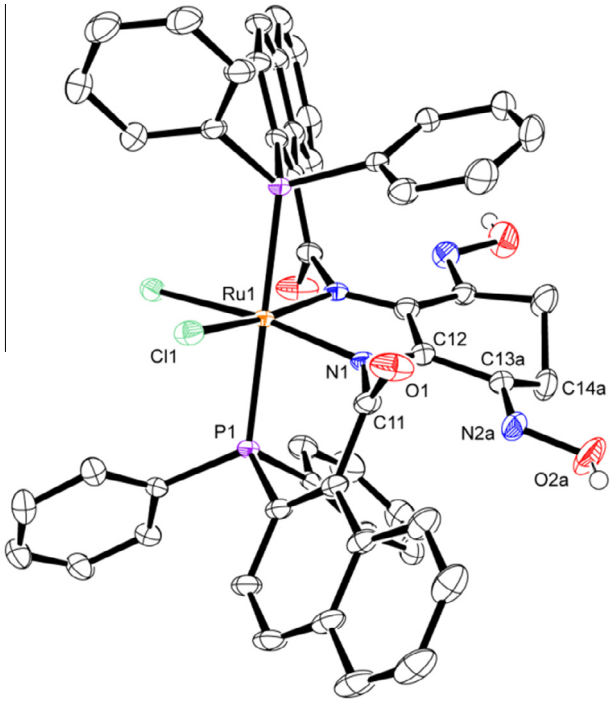

Fig. 3. Molecular structure of Ru((HON)$_2$-DACH-Naph)Cl$_2$ (**4**) showing ellipsoids at the 50% probability level and atom labeling scheme. H atoms, except those of the iminoalcohol (oxime) moieties, are omitted for clarity.

ruthenium metal center is octahedral. In comparison with other reported Ru-diimine complexes, the Ru–N bond lengths of **4** (Ru–N = 1.999 Å) lie in the observed range (Ru–N: 1.96–2.00 Å). The Ru–P and Ru–Cl bond lengths of **4** (Ru–P: 2.342 Å; Ru–Cl: 2.413 Å) and those of Ru(dppQ)Cl$_2$ and its nitration product (NO$_2$-dppQ)Ru(Cl)$_2$ reported by Mascharak [17a] (Ru–P: 2.336–2.369 Å; Ru–Cl: 2.395–2.409 Å) are also consistent with each other. Of note, **4** contains the *cis*-coordination of chloride ligands and *trans*-spanning phosphines similar to those found in Mascharak's Ru(dppQ)Cl$_2$ and (NO$_2$dppQ)Ru(Cl)$_2$ complexes, which is in contrast to that of (*R*,*R*)-**2**. It is plausible that the torsional flexibility of the diaminocyclohexyl backbone in (*R*,*R*)-**2** may allow for decreased steric congestion around the Ru center as compared to the more rigid, planar diimine complexes, thus allowing for the larger phosphine groups to maintain a cis-geometry in a tetradentate plane around Ru.

The solution state structure of **4** was consistent with the solid state structure. The C_2-symmetric nature of the complex in solution was confirmed by the number of signals observed, being half of that expected for an asymmetric system, along with the single peak observed in the ^{31}P NMR at 24.8 (s). Proton assignments were determined via multinuclear NMR experiments. Analysis of the ^{1}H NMR data of **4** indicated the loss of chirality in the cyclohexyl backbone and formation of the oxime groups (Fig. 2B). The absence of proton signal Ha, observed at δ 4.29 for (*R*,*R*)-**2** (Fig. 2A), indicated the loss of chirality and the absence of proton signals H$_b$ and H$_c$ (observed at δ 2.88 and 1.45) in (*R*,*R*)-**2** indicated the oxime formation; only signals for the diastereotopic methylene protons (H$_{f'}$: δ 2.15, overlap with DMF solvate) on the carbons adjacent to the oxime moieties (Fig. 3: C14) are observed. The oxime moieties were identified by the observation of the proton signal of the oxime (C=N–O–*H*) at δ 9.35, consistent with other reported chemical shifts for oximes [24]. As was observed in (*R*,*R*)-**2**, and the aforementioned Pt((*R*,*R*)-**1**) and Pd((*R*,*R*)-**1**) complexes, the naphthyl proton (Fig. 2B: H$_{f'}$) closest to the carbonyl group is shifted downfield significantly (δ 9.02) as compared to the free ligand form (δ 7.82), indicating coordination of the nitrogen group. FTIR analysis (MeCN solution) further confirmed the oxime formation from

the characteristic [25] broad signals at 3630 and 3542 cm^{-1} (ν_{OH}) as well as those at 1677 and 1632 cm^{-1}, corresponding to the ν_{CO} and $\nu_{C=N}$ frequencies, respectively. Note the assignment of the latter two signals is based on expected peak positions but remains to be confirmed.

The formation of **4** is a result of oxidation of the *trans*-1,2,-diaminocyclohexyl moiety of the bound (*R*,*R*)-H_2**1** ligand, to a 1,2-dimininecyclohexyl ligand (Scheme 1), and nitrosylation of the backbone cyclohexyl ring to the dioxime. The oxidation of the *trans*-1,2-diaminocyclohexyl group of (*R*,*R*)-H_2**1** to a 1,2-diiminecyclohexyl group is not unprecedented as the oxidative dehydrogenation of coordinated amines to imines by metal ions is well-established including the oxidative dehydrogenation of Ru (diamine) complexes to Ru(diimine) complexes. Specifically, Brown *et al.* reported on the oxidative dehydrogenation of Ru $(bipy)_2$(DACH-Phenyl), where DACH-Ph is the phenyl analogue of the naphthyl-ring containing DACH-Naph [26]. In the latter case, the diimine was isolated on reaction of 4 equiv Ce(IV) per mole of Ru. Interestingly, addition of more than 4 equiv Ce(IV) resulted the formation of byproducts which, while not isolated or characterized further, the authors perceive to be due to further oxidation of the dimine ligand. Our attempts to prepare the proposed intermediate diimine complex (Scheme 1: **3***) via Ce(IV) oxidation of (*R*,*R*)-**2** using either $Ce(SO_4)_2$ or silica bound Ce(IV) (Cerium(IV) ethyl/butyl phosphonate Silica, POCe; PhosphonicS™) as the Ce(IV) source, were unsuccessful. While the reactions yielded a mixture of products that we were unable to isolate or confirm their identities, we believe formation of **3*** as an intermediate step is probable based on the literature precedent for similar reactions.

Like the oxidative dehydrogenation, nitrosylation of a metal-coordinated ligand is not unprecedented. Of specific relation to this work, the Ru(dppQ)Cl_2 complex undergoes nitration (NO_2 addition) at the 4-position of the 1,2-dimino-3,5-cyclohexadiene backbone. The Ford group's excellent NO disproportionation studies on Fe(II) and Ru(II) porphyrins have established that disproportionation leads to the formation of NO_2, N_2O_3, and other reactive NO-derived compounds [27]. Based on these studies, and their own investigations, the Mascharak group has proposed that NO disproportionation of a Ru–NO species occurs in the presence of excess NO, and absence of O_2, with the resulting released NO_2 reacting with the ligand backbone in the observed nitration reaction. However, there was no evidence of **4** facilitating NO disproportionation of NO^+, which may not be unexpected owing to the lack of electrons as compared to NO.

To account for the formation of **4**, we propose the mechanism detailed in Scheme 1; beginning with the initial oxidation of the *trans*-1,2-diaminecyclohexyl group of (*R*,*R*)-**2** to form [Ru(DICH-Naph)Cl_2] (**3***; DICH = 1,2-diiminocyclohexyl) and the subsequent nitrosylation of the now activated cyclohexyl backbone at the allylic carbon centers to produce **4**. Such a mechanism explains the presence of the numerous products observed on reaction of (*R*,*R*)-**2** with [NO][BF_4] in a 1:1 ratio as formation of **4** requires a formal 4 electron oxidation and 2 equiv of NO. With only 1 equiv of [NO][BF_4] added, products from incomplete ligand oxidation resulting in monoimine-monoamine complexes are expected, along with possible nitrosylation of these complexes to form mono-oxime derivatized complexes. Formation of some amounts of **3*** and **4** are expected as well, depending on the rates of reaction. As noted earlier, attempts to isolate **3*** have been unsuccessful to this point when trying to react (*R*,*R*)-**2** with oxidants, including stoichiometric quantities of [NO][BF_4] or Ce(IV), leading to numerous oxidation products based on ^1H and ^{31}P NMR analyses. Of note, a mechanistic pathway that includes a repeated sequence of mono amido-to-imino oxidation followed by ligand backbone mono-nitrosylation cannot be discounted. Further kinetic and other mechanistic studies are required to confirm the mechanism of reaction.

4. Conclusions

Reaction of H_2**1** with $Ru(ClO_4)_2$ has allowed for the synthesis of an unoxidized, neutral diamidato, enantiopure, bis(phosphine) Ru (II) complex ((*R*,*R*)-**2**); characterized in both the solution and solid state. NMR and X-ray crystallographic studies have confirmed that the complex has structural similarities to the Pd(II) and Pt(II) complexes of $\mathbf{1}^{2-}$ and those of the Trost series of ligands with square planar tetradentate coordination, which is in contrast to the neutral complex (Ru(dppQ)Cl_2) reported by Mascharak where the phosphines coordinate trans to each other; axial to the diimine coordination. Similar to the reaction of Mascharak's Ru(dppQ)Cl_2 complex with NO that produced ligand nitrosylation, reaction of (*R*,*R*)-**2** with [NO][BF_4] did not produce the desired Ru-NO complex but rather a diamido-bis(phosphine) ligand oxidation-nitroslyation was observed yielding the interesting diiminodioxime-bis(phosphine) complex **4**. Future studies of diamido-bis(phosphine) ruthenium complexes reacting with nitric oxide sources will be of interest to determine the properties that favor the formation of stable Ru–NO complexes (e.g. Mascharak's dicarboxamide tetradentate N_4-based ligands) [28] with potential as metal-based NO-sensors, -scavenger, or NO site-specific NO delivery systems to cellular targets versus systems that undergo continued oxidation and/or nitroslyation of coordinated ligands.

Acknowledgments

The authors would like to acknowledge Grant R. Ferrell for his excellent work on the initial preparation of (*R*,*R*)-**2**. Financial support from the NSF (NSF-RUI: CHE-0809266; NSF-MRI: 1126585) and the University of San Diego is gratefully acknowledged.

Appendix A. Supplementary data

CCDC-1445800 ((*R*,*R*)-**2**) and CCDC-1445801 (**4**) contain the supplementary crystallographic data for this paper. These data can be obtained free of charge from The Cambridge Crystallographic Data Centre via www.ccdc.cam.ac.uk/data_request/cif. Supplementary data associated with this article can be found, in the online version, at http://dx.doi.org/10.1016/j.ica.2016.06.001.

References

[1] L.J. Ignarro, Nitric Oxide: Biology and Pathobiology, Academic Press, San Diego, CA, 2000.
[2] S. Kalsner (Ed.), Nitric Oxide Free Radicals in Peripheral Neurotransmission, Birkhauser, Boston, MA, 2000.
[3] J.M. Fukuto, D.A. Wink, Met. Ions Biol. Syst. 36 (1999) 547–595.
[4] G.Y. Ko, F.C. Fang, Nitric Oxide and Infection, Kluwer Academic/Plenum Publishers, New York, 1999.
[5] J. Lincoln, G. Burnstock, Nitric Oxide in Health and Disease, Cambridge University Press, New York, 1997.
[6] M. Feelisch, J.S. Stamler (Eds.), Nitric Oxide Research, John Wiley and Sons, Chichester, U.K., 1996.
[7] P.G. Wang, T.B. Cai, N. Taniguchi, Nitric Oxide Donors for Pharmaceutical and Biological Applications, Wiley-VCH, Weinheim, Germany, 2005.
[8] (a) J.A. Hrabie, L.K. Keefer, Chem. Rev. 102 (2002) 1135–1154;
(b) L.K. Keefer, Curr. Top. Med. Chem. 5 (2005) 625–636;
(c) H.H. Al-Sádoni, A. Ferro, Rev. Med. Chem. 5 (2005) 247–254;
(d) C.S. Degoute, Drugs 67 (2007) 1053–1076.
[9] (a) C. Napoli, L.J. Ignarro, Annu. Rev. Pharmacol. Toxicol. 43 (2003) 97–123;
(b) P.G. Wang, M. Xian, X. Tang, X. Wu, X. Wen, T. Cai, A.J. Janczuk, Chem. Rev. 102 (2002) 1091–1134;
(c) K. Wang, W. Zhang, M. Xian, Y.-C. Hou, X.-C. Chen, J.-P. Cheng, P.G. Wang, Curr. Med. Chem. 7 (2000) 821–834.
[10] T. Nagano, T. Yoshimura, Chem. Rev. 102 (2002) 1235–1270.
[11] M.H. Lim, S.J. Lippard, Acc. Chem. Res. 40 (2007) 41–51.
[12] C.J. Marmion, B. Cameron, C. Mulcahy, S.P. Fricker, Curr. Top. Med. Chem. 4 (2004) 1585–1603.
[13] F.G. Marcondes, A.A. Ferro, A. Souza-Torson, M. Sumitani, M.J. Clarke, D.W. Franco, E. Tfouni, M.H. Krieger, Life Sci. 70 (2002) 2735–2752.
[14] M.J. Rose, P.K. Mascharak, Curr. Opin. Chem. Biol. 12 (2008) 238–244.

[15] (a) P.C. Ford, I.M. Lorkovic, Chem. Rev. 102 (2002) 993–1017;
(b) P.C. Ford, J. Bourassa, K. Miranda, B. Lee, I. Lorkovic, S. Boggs, S. Kudo, L. Laverman, Coord. Chem. Rev. 171 (1998) 185–202.
[16] (a) N.L. Fry, P.K. Mascharak, Acc. Chem. Res. 44 (2011) 289–298;
(b) M.J. Rose, P.K. Mascharak, Curr. Opin. Chem. Biol. 12 (2008) 238–244.
[17] (a) N.L. Fry, M.J. Rose, C. Nyitray, P.K. Mascharak, Inorg. Chem. 47 (2008) 11604–11610;
(b) L. Chahen, L. Karmazin-Brelot, G. Süss-Fink, Inorg. Chem. Comm. 9 (2006) 1151;
(c) S. Burger, B. Therrien, G. Süss-Fink, Euro. J. Inorg. Chem. 17 (2003) 3099.
[18] Bruker, APEX2, SAINT, Bruker AXS Inc., Madison, Wisconsin, USA, 2012.
[19] Bruker, SADABS, Bruker AXS Inc., Madison, Wisconsin, USA, 2001.
[20] G.M. SHELX_Sheldrick, Acta Crystallogr. C71 (2015) 3.
[21] A.L. Spek, Acta Crystallogr. D65 (2009) 148.
[22] (a) R.A. Swanson, R.S. Haywood, J.B. Gibbons, K.E. Cordova, B.O. Patrick, C. Moore, A.L. Rheingold, C.J.A. Daley, Inorg. Chim. Acta 368 (2011) 74;
(b) R.A. Swanson, B.O. Patrick, M.J. Ferguson, C.J.A. Daley, Inorg. Chim. Acta 360 (2007) 2455–2463.
[23] (a) K.G. Caulton, Coord. Chem. Rev. 14 (1975) 317;
(b) M.T. Mocella, M.S. Okamoto, E.K. Barefield, Synth. React. Inorg. Met. Org. Chem. 4 (1974) 69.
[24] E. Pretsch, P. Bühlmann, M. Badertscher, Structure Determination of Organic Compounds, fourth ed., Springer, 2009.
[25] (a) G. Socrates, Infrared and Raman Characteristic Group Frequencies: Tables and Charts, third ed., Wiley, 2004;
(b) R.A. Nyquist, Interpreting Infrared, Raman, and Nuclear Magnetic Resonance Spectra, Academic Press, 2001.
[26] G.M. Brown, T.R. Weaver, F.R. Keene, T.J. Meyer, Inorg. Chem. 15 (1976) 190.
[27] M.D. Lim, I.M. Lorkovic, P.C. Ford, J. Inorg. Biochem. 99 (2005) 151.
[28] A.K. Patra, M.J. Rose, K.A. Murphy, M.M. Olmstead, P.K. Mascharak, Inorg. Chem. 43 (2004) 4487.